Force Controlled under limb Robotics Device for Rehabilitation

Sk. Shezan Arefin[1], Nahidul Hoque Samrat[2], Md. Habibur Rahaman[2], Abdullah-Al-Mamun[2], Ridwan Adib[2], Md. Tawkir Ahamed Badhan[2], Md. Iftakher Ahmed[2]

[1]Department of Electrical Engineering and Automation, Faculty of Information Engineering, Shenyang University of Chemical Technology, Shenyang, Liaoning, China.

[2]Department of EEE, International Islamic University Chittagong, Chittagong, Bangladesh

E-mail:shezan.ict@gmail.com

Abstract— **For the maintenance the balance of a Robotics Device, we need to synthesize some parameters as follows centre of mass (COM), centre of pressure(COP), centre of gravity (COG), actuated motion, actuated pressure and actuated force (torque). This paper represents force diagram of human walking and standing related to the robotics device and proposed a force control system for robotics device's balancing during walking and standing. This control system can be effective for rehabilitation, to help various people bearing weak legs or to help those enduring from a broken leg, to walk. This can also be significant as a servitor device helping people carrying heavy loads. The main characteristic is that a paasive force balancer provides the force to preserve bodyweight. An actuator is required to shift the force during swing to stance (rehabilitaion).**

Keywords- Force, Rehabilitation, Control , Limb, Human.

I. INTRODUCTION

In the recent time, researchers began to develop interfaces to discern the intention of the lower limb disabled people and to control robots using signals from muscles, brain or muscle activities. Previous studies have been reported on the dynamic signals such as forces and moments applied to handle walker, crutches and canes to assist walking. Research in aroused Robotics devices started exactly in the late 1960s.Robots are defined as standalone anthromorphic active mechanical devices that are "held" by an operator and work in concert with the operator's movements [1]. Robots are mainly used to increase performance of able-bodied wearer (e.g. for military applications), and to help disabled people to retrieve some motion abilities. Wearable robots to assist lower limb disabled people to walk have been developed and bio/kinesthetic sensors such as EMG, gyroscope, electrogoniometer, tilt sensor and accelerometer have been used to control the Robotics. In the new organized society, the robotic device that can help the lower limb disabled walk. In order to produce a convenient Robotics for them, it needs to detect the implicit intention of the user and act accordingly [2]. However, there are little studies on sensing the natural walking intention of the user with a disabled lower limb and applying to the Robotics. The explicit walking intention is defined as a user's action for walking by user-defined as a rule's action for walking by user defined rule's mainly as start walking and stop walking and implicit walking intention as user's natural physical activities (such as muscle contraction, angle of ankle or knee joint) are detected by bio/kinesthetic sensors while walking without user's explicit operation. There are several types of most famous lower limbs Robotics newer, such as:

- The BLEEX from U.C. Berkeley was designed to help soldiers to carry heavy packs.
- Rewalk developed at Haifa University, Israel, is a fully aroused electrical Robotics, allowing paraplegic people to walk using crutches [3].
- HAL-3 developed at Tsukuba University is targeted for both Performance augmenting and rehabilitative purposes [4].

The motto of this study is to describe the control of Balancing and triggering method of lower limb Robotics by using force sensor, FSR, Pressure sensor and Gyro. Force sensing resistor is a material whose resistance changes when a force or pressure is applied. We can use a single force balancer coupled for the two legs. The FSR mechanism can be relevant for the sit-to-stand, stand-to-sit, walking, and stair climbing etc for the lower limb Robotics [5].

II. METHODOLOGY:

Force Diagram: A force diagram is simply a diagram showing all the forces acting on an object, the forces direction and its magnitude. It is a simplification of the picture that shows just the forces [6]. The common diagram of three-dimensional active forces is given in figure 1.

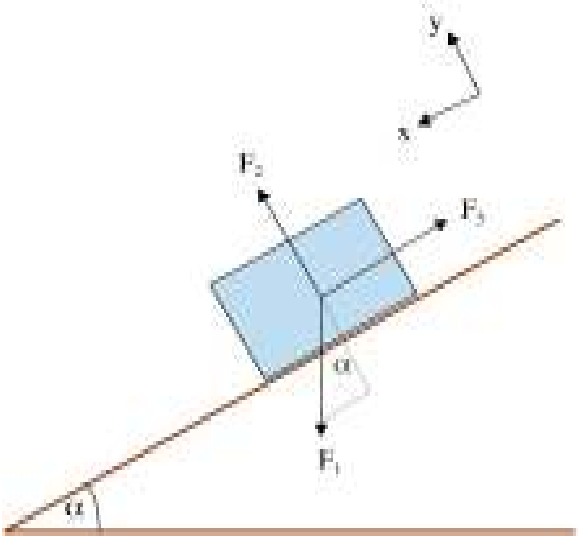

Figure 1[7]: prospective diagram of three-dimensional active forces.

If we consider three-dimensional forces applying on a free body such as: F_x, F_y and F_z instead of F_1, F_2 and F_3, we can get different momentum [8]. Moreover, Torque is the tendency of a force to rotate and object about an axis, fulcrum or pivot. The presentation and relation between torque and angular momentum is given in figure 2 [9].

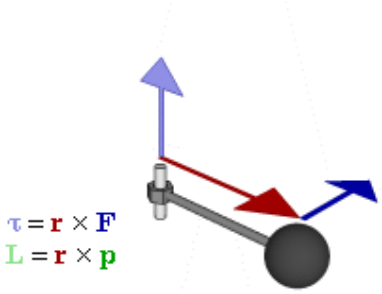

Figure 2 [10]: presentation of torque and angular momentum.

If r is the displacement vector, F is the force vector, τ is the torque, and we can get from the definition of torque:

$$\tau = r \times F \quad (1)$$

Again, if r is the particle's position vector, F is t force acting on the particle and the magnitude τ of the torque is given by

$$\tau = rF\sin\theta \quad (2)$$

Now, if we consider three axis the torque will be different in the three different ways such as:

$$\tau_1 = rF_x\sin\theta \quad (3)$$

$$\tau_2 = rF_y\sin\theta \quad (4)$$

$$\tau_3 = r\,F_z\sin\theta \quad (5)$$

The unbalanced torque on a body along axis of rotation determines the rate of change of the body's angular momentum,

$$\tau = \quad (6)$$

Where L is the angular momentum vector and t is time [9]. If multiple torques are acting on the body, it is instead the net torque, which determines the rate of change of the angular momentum:

$$\tau_1+\tau_2+\tau_3+\ldots\ldots\ldots\ldots+\tau_n=\tau_{net}= \quad (7)$$

For rotation about a fixed axis,

$$L=I\omega \quad (8)$$

Where I moment of Inertia and ω is the angular velocity.

On this section, we will work with three different circumstances sequentially "start walking" (right or left foot), "keep walking", and "stop walking" -based on tripped walking model [11]. We developed a balancing control model to recognize a user's walking intention using Force Sensing Resistor Sensors. The FSR sensor is round-shaped, diameter is 45mm, height is 16mm and weight is 0.0917kg, model no Mini45, maximum allowable overload values are 5.7 to 25.3 times rated capacities. This sensor is working in six axes.

III. Control and Balancing Method

We can describe the mechanism of FSR in two modules, sequentially: Shoe insoles sensor module: The shoe-insoles sensor module find out the walking perceptions using two FSR sensors for each foot [12]. The module receives analog signals from the two sensing ankles, converts these signals into digital signals by the Matlab-2013, which is defined by Mathworks. This has simulink toolbar, A/D converter and transmits the signals to the host module using the Plot toolbar in MATLAB. A first calibration was performed to evaluate the precision and accuracy of the sensor with static loads, with the sensor in contact with the user [13]. The calibration was performed on each subject, with the right leg in the vertical resting position, with the foot fixed to the ground. The subjects were asked not to move, and incremental torque steps ranging from −50 Nm to +50 Nm were applied to the hip joint. The subjects we choose are clearly not representative of the population meant for the rehabilitation protocols for which this Robotics is used. However, our objective was not to replicate or represent a typical rehabilitation protocol and its population, but rather to test a measurement system on a small pool of subjects [14].

Figure 3 shows the sequential procedure of controlling the balancing by FSR sensors.

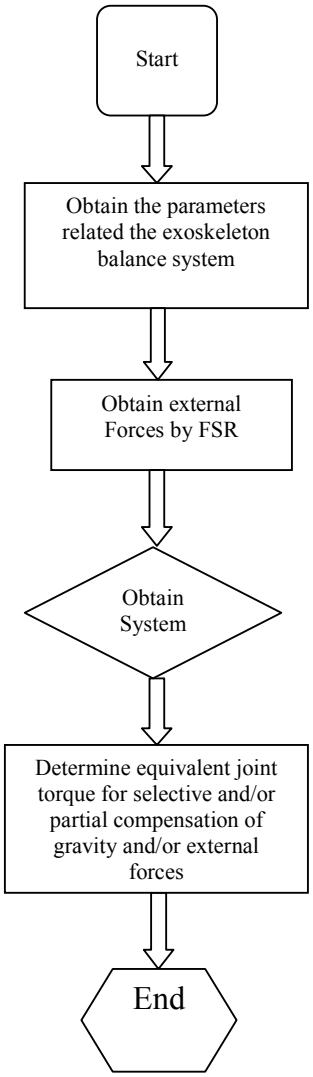

Figure 3: Operation flowchart of the FSR mechanism.

Host module: The host module transmits FSR data obtained from the above sensing modules to personal Computer. The interface between the module and personal computer is USB type [15].

Control Operation and Mechanism: To estimate the force and pressure distribution acting on the sensor from the eight voltage outputs, we implemented a simple estimation algorithm, which uses the model of sensor derived with the characterization described in the previous section. This algorithm is based on the assumption that the force and voltage of each of the eight sensitive elements is not correlated with that of the other neighboring elements [16]. This is a simplification: the deformation of one element depends on the deformation of the neighboring elements because the silicone cover is a single structure. With this method, it is necessary to characterize the sensor only once, under uniform loading condition. The force estimation algorithm, however, does not make the hypothesis that the load is uniformly distributed, rather, it can be used (with variable performances) under all loading conditions. The algorithm works as follows: The signals are filtered and de-offset. The eight voltages are used as input for the force/voltage models, to extract eight force values. The eight resulting forces are averaged to determine the estimated force on the sensor; (Parallel to 3) the eight resulting forces are transformed in eight pressure distribution values (dividing by the surface of the pad) [17].

Table 1. Normalized and absolute RMSE of the estimated force, and systematic measurement error compared with the load-cell force, for the three pads under the three loading conditions [18].

Similarly calculation procedure used for other two sites. So total cost per KWh for Kutubdia Island is 0.01179USD/KWh and Sandwip island 0.01064USD/KWh. It could clear that energy production cost in Sandwip Island per KWh is lower than other two sites.

	Curvature 1		**Curvature 2**	
	Systematic % Error	**RMSE [N% (N)]**	**Systematic % Error**	**RMSE [N% (N)]**
Pad 1	3.8%	7.2% (4.3)	3.4%	7.5% (4.5)
Pad 2	3.7%	2.7% (1.6)	3.3%	2.7% (1.6)
Pad 3	3.8%	7.8% (4.7)	3.4%	8.5% (5.1)

Due to the assumption made by this algorithm, the accuracy and measurement noise of the sensor depend on the loading condition, and need to be evaluated for each expected loading pattern. To give an example of the performances of the sensor, we tested it fewer than two different no uniform loading conditions. We developed two rigid indenters with a curve indentation face (two different curvatures, three m−1 and 5 m−1 were tested). We analyzed the performance of the sensors by applying loads in the range of 0 to 60 N, and by comparing the output of the force estimation algorithm with the recording of a load cell. The experimental setup was the same used in the calibration phase, as 5 loading-unloading cycles where performed at a constant speed of 1 mm/min. Figure 6 reports the estimation results for the two conditions, with a sketch of the indenter used for the purpose [19]. The blue dots represent the estimation of the algorithm, and the red line a linear fitting of the estimates. It can be seen that non-uniform loads introduce two sources of error in the estimate. Table 2 reports the normalized and absolute RMSE of the measurements to evaluate measurement noise, as well as the systematic error of the sensor. The normalized RMSE was calculated comparing the estimated force with the load-cell force, and normalizing with the full-scale force of 60 N [20]. The systematic error was evaluated by linearly fitting the estimates of the pressure sensor, and by comparing the slope of the fitted curve with the ideal steepness of 1 (which corresponds to a measure with no systematic error). The maximum error introduced by this systematic effect on the measure is of about 2 N, which is well below the measurement noise as evaluated by the RMSE (which can reach 5 N) [21].

These results show that our sensory apparatus can be effectively used to monitor human robot interaction in a lower limb Robotics [22]. In controlled conditions, it has been shown that a constant fraction of interactive force unloads on each sensitive element, both in static and dynamic loading conditions. For this reason, our sensory system can be used to evaluate the resulting human-robot interaction force, providing a redundant and therefore highly reliable measurement. More than that, our sensory system allows evaluating how the interactive forces are distributed over the contact area on the user's limb. Compared to single point measures, therefore, our system provides an objective mean to evaluate the interaction comfort (in terms of local pressure on the limb), and allows to quantify the fastening force (by monitoring the preloading of each pad) on the belt. In this Section, we performed a characterization of the sensory system by comparing the output of each tactile sensor with that of a load cell. Similar results could have been obtained by comparing with a different interaction force estimate, obtained through measurements of the interaction torque. For example, model-based interaction torque estimates, or direct measurements from a reliable torque source, could have been used [23].

IV. CONCLUSION:

The article represented the force diagram and structure of human movement related to the Robotics device for human balancing. The article also introduced a force-controlled system for lower limb Robotics device's balance system and. In this paper, we described the control system and force management only for maintaining the actuated motion in order to balancing technique for walking and standing. We hope and expect that in near future we will be able to describe a relevant force-controlled system for a Robotics device in terms of stair climbing, jumping and many others application.

REFERENCES

[1] A. M. Dollar, "Lower Extremity Roboticss and Active Outhouses: Challenges and state-of-art," IEEE Transactions on Robotics, PP. 144-158, Feb 2008.

[2] O.B.J Makinson, "Research and Development Prototype for Machine Augmentation of Human Strength and Endurance, Hardiman I project Schenectady, NY," General Electric Report S-71-1056, 1971.

[3] N.J. Mizen: Preliminary design for the shoulders and arms of a powered, Robotics structure, cornell aeronaut.lab. Rep. V0-1692-v-4(1965)

[4] Pons, J. L. Rehabilitation Robotics robotics. The promise of emerging field. IEEE Eng. Med. Biol. Mag. 2010, 29, 57-63

[5] K. H. Low, Xiaopeng Liu, and Haoyong Yu, "Development of NTU wearable Robotics System for Assistive Technologies," Proceedings of the IEEE International Conference on Mechatronics & Automation, July 2005, pp. 1099-1106.

[6] H. Kazerooni, "Roboticss for human performance augmentation", A Chapter in book: Robotics Handbook, Springer-Verlag, 2008.

[7][Online: March 2014] "Free body diagram of a mass on a slope", http:// www.ffden-2.phys.uaf.edu.

[8] Mone G. Building the real Iron man. Popular Science/http://www.popsci.com/. April 2008.

[9] J. D. Millan, F. Renkens, J. Mourino and W. Gerstner, "Noninvasive brain-actuated control of a mobile robot by human EEG", IEEE Transactions on Biomedical Engineering, Vol. 51, pp. 1026-1033, 2004.

[10][Online: March 2014] "Torque and Force", http://en.wikipedia.org/wiki/Torque.

[11] H. Kawamoto and Y. Sanki, "Power assist system HAL-3 for gait disorder person", in proc. Int. Conf. Comput. Helping people Special Needs (ICCHP) (Lecture Notes on Computer Science), vol. 2398, Berlin, Germany: Spinger-Verlag, 2002.

[12] M. Raibert and J. Craig. Hybrid position/force control of manipulators. ASME Journal of Dynamic Systems, Measurement and Control, 102(2): 126-133, 1981.

[13][Online: April 2014] "Free body diagram of an Robotics leg", http://www.dynamicsystems.asmedigitalcollection.asme.org.

[14] Okubo J, Watanabe I, Takeya T, Baron JB. Influence of foot position and visual field condition in the examination of equilibrium function and sway of centre of gravity in normal persons. Agressologie 1979; 20:127-32.

[15] Ferris DP, Czerniecki JM, Hannaford B. An ankle-foot orthosis powered by artificial pneumatic muscles. Journal of Applied Biomechanics May; 2005 21:189-197. [PubMed: 16082019].

[16] A. Goffer, "Gait-locomotor Apparatus," European patent EP1260201 (A1), Argo Medical Technologies LTD, November 27, 2002.

[17] Guizzo, E.; Goldstein, H. The rise of the body bots. IEEE Spectrum 2005, 42, 50-56.

[18] General Electric Co. Hardiman I Prototype Project, Special Interim Study; Report S-68-1060; General Electric Co.: Schenectady, NY, USA, 1968.

[19] Zoss, A.B.; Kazerooni, H.; Chu, A. Biomechanical design of the Berkeley lower extremity Robotics (BLEEX). IEEE ASME Trans. Mechatron. 2006, 11, 128-138.

[20]Suzuki, K.; Mito, G.; Kawamoto, H.; Hasegawa, Y.; Sankai, Y. Intention-based walking support for paraplegia patients with robot suit HAL. Adv. Robot. 2007, 21, 1441-1469.

[21]Jezernik, S.; Colombo, G.; Keller, T.; Frueh, H.; Morari, M. Robotic orthosis lokomat: A rehabilitation and research tool. Neuromodulation 2003, 6, 108-115.

[22] Bergamasco, M.; Allota, B.; Bisio, L.; Ferretti, L.; Parini, G.; Prisco, G.M.; Salsedo, F.; Sartini, G. An arm Robotics system for teleoperation and virtual environments applications. In Proceedings of IEEE International Conference on Robotics and Automation, San Diego, CA, USA, 08–13 May 1994; pp. 1449-1454.

[23] Stefano Marco Maria De Rossi , Nicola Vitiello , Tommaso Lenzi , Renaud Ronsse , Bram Koopman , Alessandro Persichetti , Fabrizio Vecchi , Auke Jan Ijspeert , Herman van der Kooij and Maria Chiara Carrozza, " Sensing Pressure Distribution on a Lower-Limb Robotics Physical Human-Machine Interface" , Sensors 2011, 11, 207-227; doi:10.3390/s 110100207.